Geophysical Research Letters

RESEARCH LETTER
10.1029/2025GL116531

Direct Assimilation of Radar Reflectivity Data in Logarithmic Scale or Power Transform?

Peng Liu[1,2], Guifu Zhang[1,2], Jacob T. Carlin[3], and Jidong Gao[3]

[1]School of Meteorology, University of Oklahoma, Norman, OK, USA, [2]Advanced Radar Research Center, University of Oklahoma, Norman, OK, USA, [3]NOAA/OAR National Severe Storms Laboratory, Norman, OK, USA

Key Points:

- The direct assimilation of power-transformed reflectivity data instead of its typical logarithmic scale is proposed
- Experiments of direct assimilation of logarithmic and power-transformed reflectivity data are conducted and their performance is assessed
- The new direct assimilation of power-transformed radar reflectivity outperforms that of the radar reflectivity on a logarithmic scale

Supporting Information:

Supporting Information may be found in the online version of this article.

Correspondence to:

P. Liu,
Peng.Liu-1@ou.edu

Citation:

Liu, P., Zhang, G., Carlin, J. T., & Gao, J. (2025). Direct assimilation of radar reflectivity data in logarithmic scale or power transform? *Geophysical Research Letters*, *52*, e2025GL116531. https://doi.org/10.1029/2025GL116531

Received 21 MAY 2025
Accepted 21 SEP 2025

Author Contributions:

Conceptualization: Peng Liu, Guifu Zhang
Investigation: Peng Liu, Jacob T. Carlin, Jidong Gao
Methodology: Peng Liu, Guifu Zhang, Jidong Gao
Project administration: Guifu Zhang
Validation: Peng Liu
Visualization: Peng Liu
Writing – original draft: Peng Liu
Writing – review & editing: Peng Liu, Guifu Zhang, Jacob T. Carlin, Jidong Gao

Abstract To cover its large dynamic range, radar reflectivity factors have historically been displayed and used on a logarithmic scale, that is, decibels of reflectivity (dBZ). Logarithmic reflectivity has also been used for data assimilation without being questioned or well validated. However, fundamental limitations exist with directly assimilating logarithmic reflectivity, such as strong nonlinearity of the observation forward operator and the fact that the impacts of small reflectivity values are amplified, leading to exaggerated increments when mapped back into physical space. In this study, we power-transform both reflectivity and hydrometeor mixing ratios to alleviate the aforementioned issues with using conventional logarithmic reflectivity. Forecast evaluation across eight severe convection events demonstrates that applying the Box-Cox power transformations to both reflectivity and hydrometeor mixing ratios effectively reduces the nonlinearity between the observations and control variables. This approach significantly improves analyses of model hydrometeor variables and forecasts of composite reflectivity and hourly precipitation.

Plain Language Summary Owing to its huge dynamic range spanning many orders of magnitude, reflectivity from weather radars is typically presented in a logarithmic scale. However, using this data in a logarithmic scale to update numerical weather models introduces several fundamental issues that may undermine its potential benefits, including inflating the adjustments from low reflectivity values and exacerbating the complex relationship between reflectivity and model variables. In this study, we use a new power transformation to scale the reflectivity, partially mitigating some of the problems introduced by the conventional logarithmic approach and improving the prediction of severe thunderstorms.

1. Introduction

Convective-scale numerical weather prediction (NWP) is very sensitive to initial and boundary conditions. Doppler weather radar is a primary observational data source for the convective scale. As such, assimilation of high-density radar observations, such as radial velocity (v_r) and radar reflectivity at horizontal polarization (Z_h in $mm^6\ m^{-3}$ or $Z_H = 10\log(Z_h)$ in dBZ), to improve the initial conditions of NWP models has led to impressive achievements over two decades (Gao et al., 2024). Radial velocity v_r can be assimilated more easily and directly than Z_h due to the linear relation between v_r and the model wind components. Radar reflectivity measures the power scattered by hydrometeors, but the high degree of nonlinearity between the Z_h and model hydrometeor control variables (mixing ratios q and number concentrations N_t) of multiple species leads to more complexity and difficulty in directly assimilating reflectivity using a forward observation operator. Some studies have attempted to achieve indirect assimilation of reflectivity by first retrieving the intermediate variables (e.g., hydrometers, water vapor, vertical velocity) and then assimilating them (Gan et al., 2023; Lai et al., 2019; Wang et al., 2013). However, indirect assimilation is very sensitive to the retrieval procedure which can have significant errors.

To directly assimilate radar reflectivity into NWP models, accurate and efficient forward operators that link model variables to Z_h are needed (Gao & Stensrud, 2012; Jung et al., 2008; Tong & Xue, 2005; Zhang et al., 2021). However, most previous studies have focused more on the development of advanced assimilation methods and less on the radar forward operators and the representation of reflectivity in NWP models. The forward operators used in most studies directly assimilating radar reflectivity are based on the Rayleigh scattering approximation, which requires particle sizes much smaller than the radar wavelength (e.g., $D < \lambda/16$) (Zhang, 2016). In addition, only rain and dry ice species (snow, graupel, and/or hail) are considered, while the mix-phased species (e.g., wet snow) that contribute more to reflectivity and have significant radar features (e.g., bright band) are either ignored or inaccurately calculated (Blahak, 2016; Jung et al., 2008; Wolfensberger &

Berne, 2018). Zhang et al. (2021) developed a set of parameterized forward operators (PFOs) to improve the accuracy of calculated radar variables based on rigorous scattering calculations performed using the T-matrix method. Liu, Zhang, et al. (2024) implemented a new continuous melting model into these parameterized forward operators to enhance the radar representation of mixed-phased species. The new PFOs with the continuous melting model resulted in superior analyses and forecasts when used to directly assimilate Z_h compared to the widely used power-law forward operators based on the Rayleigh scattering approximation (Liu, Gao, et al., 2024). However, there is still a lot of room for improvement of radar forward operators to enhance the direct assimilation of radar data.

Because Z_h spans many orders of magnitude (varying from less than 1 $mm^6\ m^{-3}$ up to more than $10^7\ mm^6\ m^{-3}$), the radar meteorology community typically represents it on a logarithmic scale $Z_H = 10\log(Z_h)$. The data assimilation and NWP communities also use Z_H in forward observation operators. This logarithmic representation amplifies the contribution of small or no-precipitation reflectivity during the minimization process and easily produces spurious cells in the analysis. To prevent this, a threshold of 5–15 dBZ is usually set to filter out regions of low Z_H (Aksoy et al., 2009; Gao et al., 2016; Janjić & Zeng, 2021). A lower threshold tends to increase the amount of spurious convection, while a higher threshold risks losing important observational information, especially for nascent convective storms. The high nonlinearity of the forward operator is also a major challenge for assimilating Z_H. Some studies have applied a power transformation to the hydrometeor control variables to adjust their range and distribution shape and accelerate minimization convergence, with demonstrated improved performance (Chen et al., 2021; Hu et al., 2023). However, the power-transformed hydrometeor control variables still have a complicated nonlinear relationship with Z_H.

To further improve reflectivity forward operators by reducing their nonlinearity, we propose for the first time applying a Box-Cox power transformation (Box & Cox, 1964) to Z_h instead of the logarithmic representation. In this approach, power transformations are utilized for both Z_h and the hydrometeor control variables to alleviate the high nonlinearity of the reflectivity forward operators and overcome the limitation of low reflectivity thresholds so that more information can be extracted from reflectivity observations. Herein, the impact of this reduction in observation operator nonlinearity is assessed for short-term forecasts of eight high-impact convection events using the newly developed reflectivity PFOs within a 3DVAR framework. The data and methods are described in Section 2. The analysis and forecast evaluation are presented in Section 3. A summary and discussion are provided in Section 4.

2. Methodology

2.1. Direct Assimilation of Radar Reflectivity

2.1.1. Calculation of Radar Reflectivity Factor

Prior to any transformation, the direct assimilation of reflectivity requires the calculation of Z_h from model state variables. In most previous studies, Z_h is calculated as the sixth moment of the drop size distribution for rain and is proportional to the sixth moment of the particle size distribution (PSD) for other species assuming Rayleigh scattering, taking into account the presumed hydrometeor density. However, as described previously, Liu, Gao, et al. (2024) demonstrated that the T-matrix-derived PFOs of Zhang et al. (2021) are more accurate and efficient for directly assimilating reflectivity. Herein, we use these PFOs to calculate the Z_h of each hydrometeor species x for both the logarithmic and power-transformed schemes to more readily isolate the effects of the applied transformations.

In the PFO for rain, $Z_h(r)$ is fitted to polynomial functions of mass/volume-weighted mean diameters (D_m, mm) and liquid water content $W = \rho_a q_r$ ($g\ m^{-3}$), where ρ_a ($kg\ m^{-3}$) and q_r ($g\ kg^{-1}$) are the air density and mixing ratio of rain, respectively, following Mahale et al. (2019):

$$Z_h(r) \approx W\left(-0.3078 + 20.87D_{m,r} + 46.04D_{m,r}^2 - 6.403D_{m,r}^3 + 0.2248D_{m,r}^4\right)^2. \quad (1)$$

For a given ice and mixed-phase species x (such as snow, graupel, and hail), $Z_h(x)$ is parameterized as a polynomial function of D_m and the percentage of melting (f_{mx}), as follows:

$$Z_{\mathrm{h}}(x) \approx Z_x\left[a_{Z0}\left(f_{mx}\right) + a_{Z1}\left(f_{mx}\right)D_{m,x} + a_{Z2}\left(f_{mx}\right){D_{m,x}}^2 + a_{Z3}\left(f_{mx}\right){D_{m,x}}^3\right]^2, \quad (2)$$

where a_Z are fitting coefficients detailed in Tables 1–3 of Zhang et al. (2021). The f_{mx}, mixing ratio, and number concentration of each melting species are estimated from the melting model (Liu, Zhang, et al., 2024). In Equation 2, Z_x is equal to the sixth moment of the PSD, as follows:

$$Z_x \equiv M_{6x} = 11.25 \times 10^3 \frac{\rho_a q_x}{\pi \rho_x} {D_{m,x}}^3, \quad (3)$$

where ρ_x (g cm^{-3}) and q_x (g kg^{-1}) are the density and mixing ratios for ice and melting species, respectively.

2.1.2. Traditional Reflectivity Logarithmic Assimilation Scheme

In all previous direct assimilation studies, the radar reflectivity factors Z_{h} (mm^6 m^{-3}) for each hydrometeor species x are summed and converted to a logarithmic-scale Z_{H} (dBZ),

$$Z_{\mathrm{h}} = \sum Z_{\mathrm{h}}(x), \quad (4)$$

$$Z_{\mathrm{H}} = 10 \log(Z_{\mathrm{h}}), \quad (5)$$

and used within the assimilation scheme.

2.1.3. New Reflectivity Power-Transform Assimilation Scheme

Yang et al. (2020) proposed applying the Box-Cox power transformation (Box & Cox, 1964) within a variational framework. Subsequently, this transformation was extended to hydrometeor control variables including mixing ratio and number concentration, as well as water vapor mixing ratio, in order to adjust their dynamic ranges (Chen et al., 2021; Hu et al., 2023; Li et al., 2022). We propose a new radar reflectivity direct assimilation approach that simultaneously applies this power transformation to Z_{h} and the control variables to alleviate the high nonlinearity between the observations and model state variables. The power-transformed radar reflectivity factors $\tilde{Z}_{\mathrm{h}}$ and control variables $\tilde{q}$ are calculated as follows:

$$\tilde{Z}_{\mathrm{h}} = \left(Z_{\mathrm{h}}^{p_z} - 1\right)/p_z, \quad (6)$$

$$\tilde{q} = \left(q^{p_q} - 1\right)/p_q, \quad (7)$$

where p_z and p_q represent the transform parameters for reflectivity and hydrometeor mixing ratios, respectively, that are larger than zero but do not exceed 1. Chen et al. (2021) and Hu et al. (2023) demonstrated that $p_q = 0.4$ yields the best analyses for convective storm structures; thus, $p_q = 0.4$ is used here. Because Z_{h} and hydrometeor mixing ratios are proportional to approximately the sixth and third moments of the PSD, respectively, the most linear relation should be achieved when p_z is about half of p_q. We performed a set of sensitivity experiments to test the impact of two p_z values: 0.1 and 0.2. The results indicated that the analyses and forecasts are sensitive to the value of p_z (not shown). Overall, $p_z = 0.1$ showed the best performance for both reflectivity and precipitation forecasts for most convective events, so it is used in this study.

Simulations of a real convection event using the PFO reveals that the strongest nonlinearity exists between the logarithmic reflectivity factors and linear mixing ratios (Figures 1a1–ac1). Applying power transforms to the mixing ratios alleviates some of the nonlinearity (Figures 1a2–1c2), while the best possible approximately linear relationship is given by simultaneously applying power transformations to both the reflectivity factors and mixing ratios (Figures 1a3–1c3).

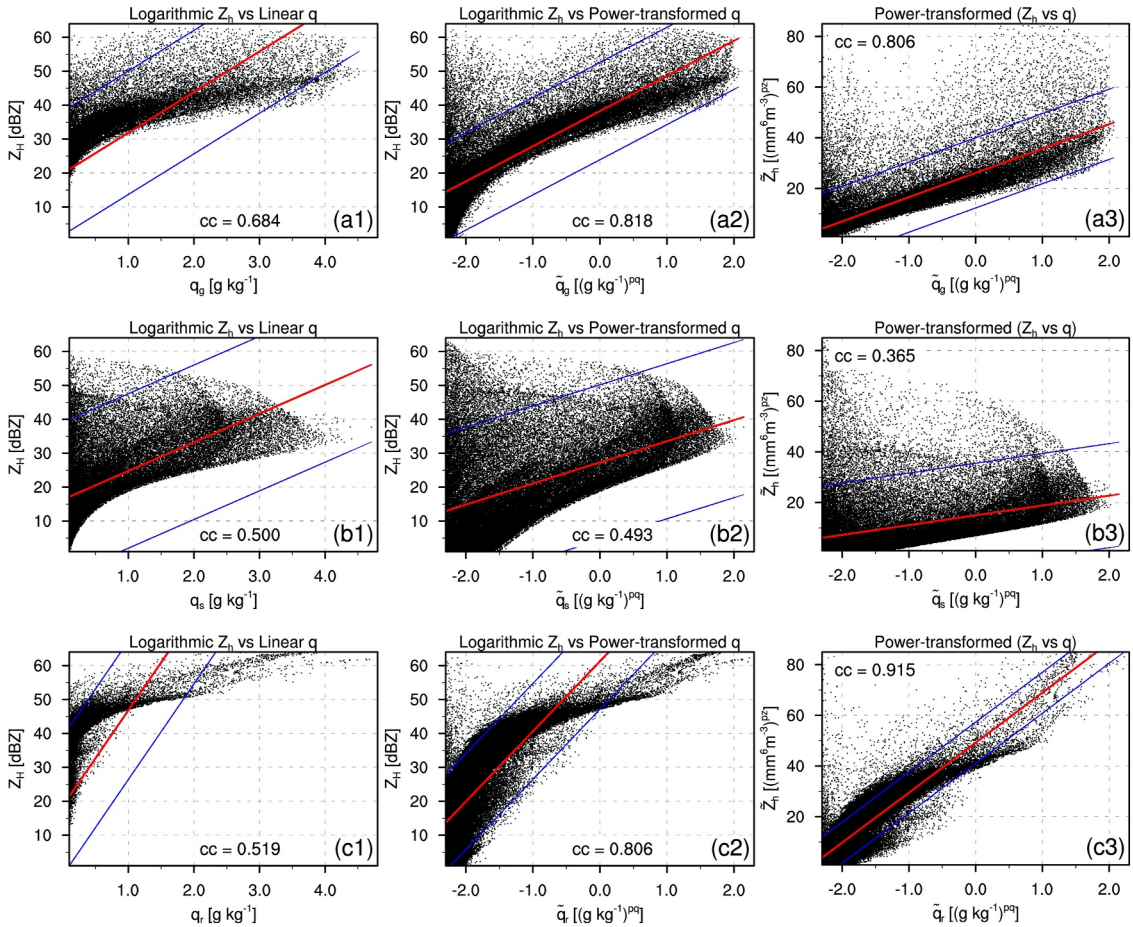

Figure 1. The mixing ratios for graupel (a1–a3), snow (b1–b3) and rain (c1–c3) versus radar reflectivity factor calculated by the PFO from simulations at 2200 UTC on 24 May 2019 for three different transformation combinations: (a1–c1) linear mixing ratios versus logarithmic reflectivity, (a2–c2) power-transformed mixing ratios versus logarithmic reflectivity, and (a3–c3) power-transformed mixing ratios versus power-transformed reflectivity. The least-squares fitted regression line and the 5th–95th percentile intervals are shown in red and blue lines, respectively. The Pearson correlation coefficients (cc) are also shown.

2.2. Experimental Design

2.2.1. Experimental Design and Model

To investigate the impact of logarithmic and power transformations on the direct assimilation of reflectivity, three distinct sets of experiments are conducted. The first set (LogZLinearQ) uses mixing ratios as control variables to assimilate logarithmic Z_H, which is the most common approach. The second set (LogZPowerQ), uses power-transformed mixing ratios as control variables to assimilate Z_H. The third set (PowerZPowerQ), uses power-transformed mixing ratios as control variables to assimilate power-transformed reflectivity factors $\tilde{Z}_h$.

In our study, eight severe convection events (01, 06, 20–24, and 28 May 2019)—see Table 1 in Liu, Gao, et al. (2024) for more details—were chosen from the 2019 National Oceanic and Atmospheric Administration (NOAA) Hazardous Weather Testbed (HWT) Spring experiment cases (Clark et al., 2020) to assess the impact of different direct assimilation schemes on short-term severe weather forecasts. The WRF model version 3.7.1 (Skamarock et al., 2008) is utilized as the forecast model, and the model driven by High-Resolution Rapid Refresh (HRRR) forecast product (Dowell et al., 2022). The model domain has 601 × 601 grid points with a 1.5-km horizontal grid spacing. The model physics configuration is described in Supporting Information S1.

2.2.2. Assimilation System Setting and Observational Data

In this study, we employed a straightforward 3DVAR assimilation approach following the methodology of Gao et al. (1999, 2004). This system, developed for high-frequency convective-scale data assimilation, has been

utilized at the Center for Analysis and Prediction of Storms (CAPS) and the National Severe Storms Laboratory (NSSL) for many years (Gao, 2017). The system can efficiently assimilate high-frequency radar data to produce timely analyses beneficial in high-impact severe weather environments (Gao et al., 2013). All assimilated radar data were NEXRAD Level-II data. Prior to assimilation, we performed rigorous quality control on the raw radar data, including radial velocity de-aliasing, removal of ground clutter, and filtering of non-meteorological and reflectivity outlier gates. For more details on the assimilation system and observational data, see Supporting Information S1.

3. Results

3.1. 24 May 2019 Analysis

To illustrate the impact of applying a power transformation to the reflectivity factor on the analysis, a detailed investigation of the 24 May case, which featured clusters of supercells, is presented. Figure 2 shows vertical profiles of the mean absolute analysis increment for the hydrometeor mixing ratios at three observed reflectivity thresholds during all assimilation cycles. Compared to the conventional assimilation scheme LogZLinearQ, the LogZPowerQ and PowerZPowerQ experiments yielded larger rain increments and produced a graupel and snow increment peak above the 20th model level (about 7.5 km). As shown in Figure 1, applying the power transformation to hydrometeor variables improves the nonlinear relationship between reflectivity and hydrometeors, resulting in larger rain and ice-phase species increments in the LogZPowerQ and PowerZPowerQ experiments. Additionally, the maximum increments for ice-phase species appear at more reasonable heights after applying the power transformation to the control variables. Comparing the logarithmic and power-transformed reflectivity assimilation schemes, both experiments show similar vertical profiles for rain and ice-phase species, but with slightly larger increments for rain and smaller increments for ice-phase species in PowerZPowerQ. This is due to the current power parameters better mitigating the nonlinearity between reflectivity and rain than ice-phase species. Interestingly, PowerZPowerQ exhibits smaller positive increments at smaller thresholds ($Z_h < 20$ dBZ) and larger positive increments at larger thresholds ($Z_h \geq 40$ dBZ) than LogZLinearQ or LogZPowerQ, while the opposite is true for negative increments. This is because the logarithmic transformation has a more pronounced amplification effect on small reflectivity values than the power transformation, leading to overestimated analysis increments, and potentially producing spurious convection when assimilating small reflectivity values.

3.2. 24 May 2019 Forecast

Figure 3 presents the analyzed and forecasted composite reflectivity for the different assimilation experiments compared to observations. At the 2200 UTC 24 May 2019 initialization, a cluster of convective cells is observed in northwest Oklahoma and southern Kansas (Region A), well-developed supercells exist in northwest Texas (Region B), and another multicell convective storm is present in west Texas (Region C) (Figure 3a0). All three analyses reproduce the observed convective cells and supercells, with some over-analysis in LogZLinearQ (Figure 3a1). By 2300 UTC, 1 hr into the forecast, LogZLinearQ exhibits significant underprediction of convection in Regions A and B (Figure 3b1), consistent with the rapid disappearance of incremental information reported in many studies of direct reflectivity assimilation using untransformed hydrometeor control variables (Hu et al., 2023). By 0000 UTC, the scattered convective cells in Region A and the multiple supercells in Region B merged and developed into a squall line (Figure 3c0). By 0100 UTC, 3 hr into the forecast, LogZLinearQ misses almost the entire portion of this squall line within Region A. LogZPowerQ performs better than LogZLinearQ but still does not predict the squall system well, with only PowerZPowerQ predicting the squall structure within Region A relatively completely. On the other hand, all the experiments fail to predict the extent of the stratiform area behind the leading convective line in Region B (Figure 3d0–3d3), a long-standing issue caused by a range of complicated model factors (Han et al., 2019; Morrison et al., 2009, 2015; Varble et al., 2014).

Neighborhood equitable threat scores (NETS) and false alarm ratios (NFAR) with a 6-km radius are calculated in Figure 4 to quantitatively assess the composite reflectivity and precipitation forecast performance at different thresholds (Clark et al., 2010; Schwartz, 2017). Larger NETS values indicate better forecast performance, while larger NFAR values signify more spurious forecasts. For composite reflectivity, LogZLinearQ shows the worst forecast performance, exhibiting the smallest NETS and the largest NFAR at various thresholds throughout the entire forecast (Figures 4a1–4b3). During the first 30 min of the forecast, NETS and NFAR for LogZPowerQ and PowerZPowerQ almost overlap, with LogZPowerQ having a slightly larger NETS at the start. This may be related

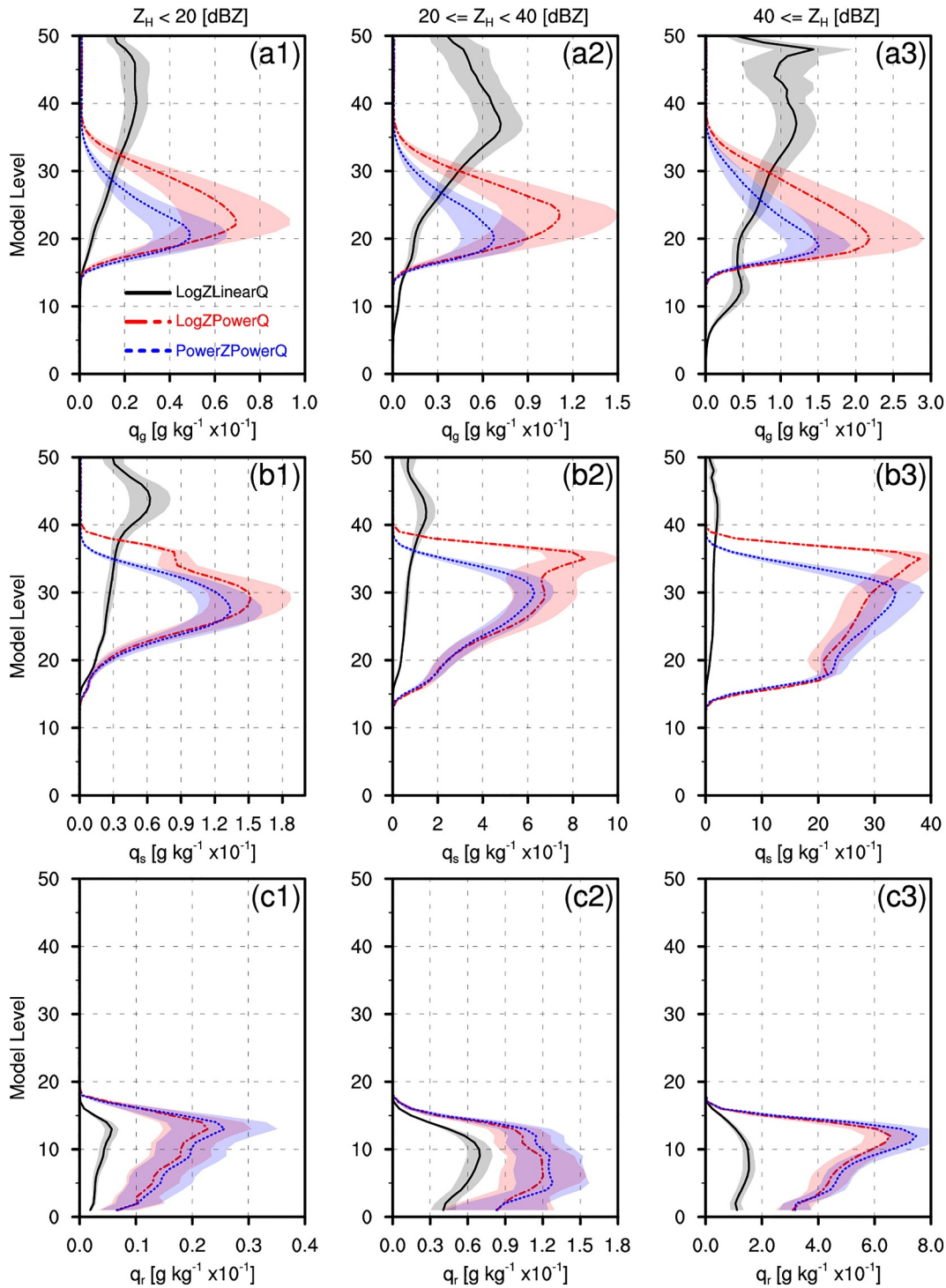

Figure 2. Vertical profiles of the absolute analysis increment mean for graupel (a1–a3), snow (b1–b3) and rain (c1–c3) mixing ratios in LogZLinearQ (black solid lines), LogZPowerQ (red dashed lines) and PowerZPowerQ (blue dashed lines) over the grid points where the observed reflectivity is $Z_H > 20$ dBZ (a1–c1), 20 dBZ $\leq Z_H < 40$ dBZ (a2–c2), and $Z_H \geq 40$ dBZ (a3–c3), averaged all assimilation cycles between 1900 and 2300 UTC on 24 May 2019. The shading in each panel indicates the 95% confidence interval.

to the larger analysis increments of ice-phase species in LogZPowerQ. The most significant improvement in PowerZPowerQ compared to LogZPowerQ occurs after 60 min, when PowerZPowerQ produces larger NETS and smaller NFAR at all thresholds, especially above 40 dBZ. Consistent with the scores for composite reflectivity,

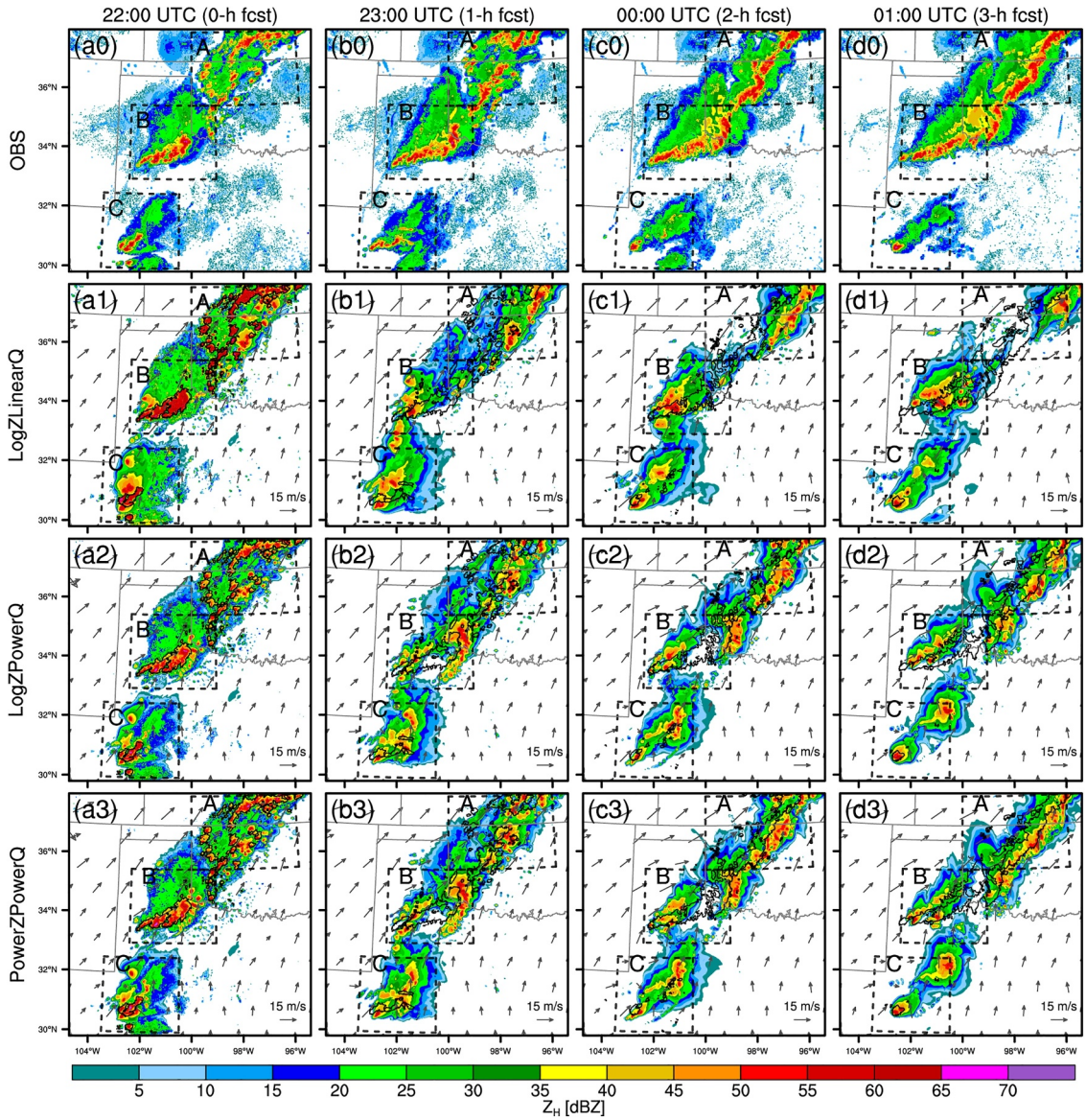

Figure 3. The observed (a0–d0), analyzed (a1–a3) and forecasted (b1–d3) composite Z_H (dBZ) and wind vectors at z = 3.0 km at 2200 UTC on 24 May (a0–a3), 2300 UTC on 24 May (b0–b3), 0000 UTC on 25 May (c0–c3), and 0100 UTC on 25 May (d0–d3), by LogZLinearQ (a1–d1), LogZPowerQ (a2–d2) and PowerZPowerQ (a3–d3) initiated at 2200 UTC. The black solid lines in panels (a1–d3) represent observed Z_H = 35 dBZ. The black dashed rectangular boxes (A, B, and C) denote regions referred to in-text.

LogZLinearQ provides the lowest precipitation forecast skill (Figures 4c1–4d3). Unlike composite reflectivity, PowerZPowerQ's improvement in precipitation compared to LogZPowerQ is sustained throughout the forecast period and is evident at all thresholds. As shown in Figures 2c1–2c3, the precipitation forecast improvement is primarily due to the adjustment of the rain mixing ratios through the power-transformed reflectivity factors. That is, applying a power transformation to the reflectivity factors alleviates the highly nonlinear relationship between the reflectivity and hydrometeor variables, allowing the influence of small reflectivity values to be retained. This avoids the amplification of small reflectivity factor values that occurs when directly assimilating logarithmic reflectivity factors. In addition, we also performed an assimilation experiment (PowerZLinearQ) in which only reflectivity was power-transformed while hydrometeor control variables remained linear. This experiment revealed a consistent improvement over LogZLinearQ in forecasting performance, similar to that of LogZPowerQ (not shown).

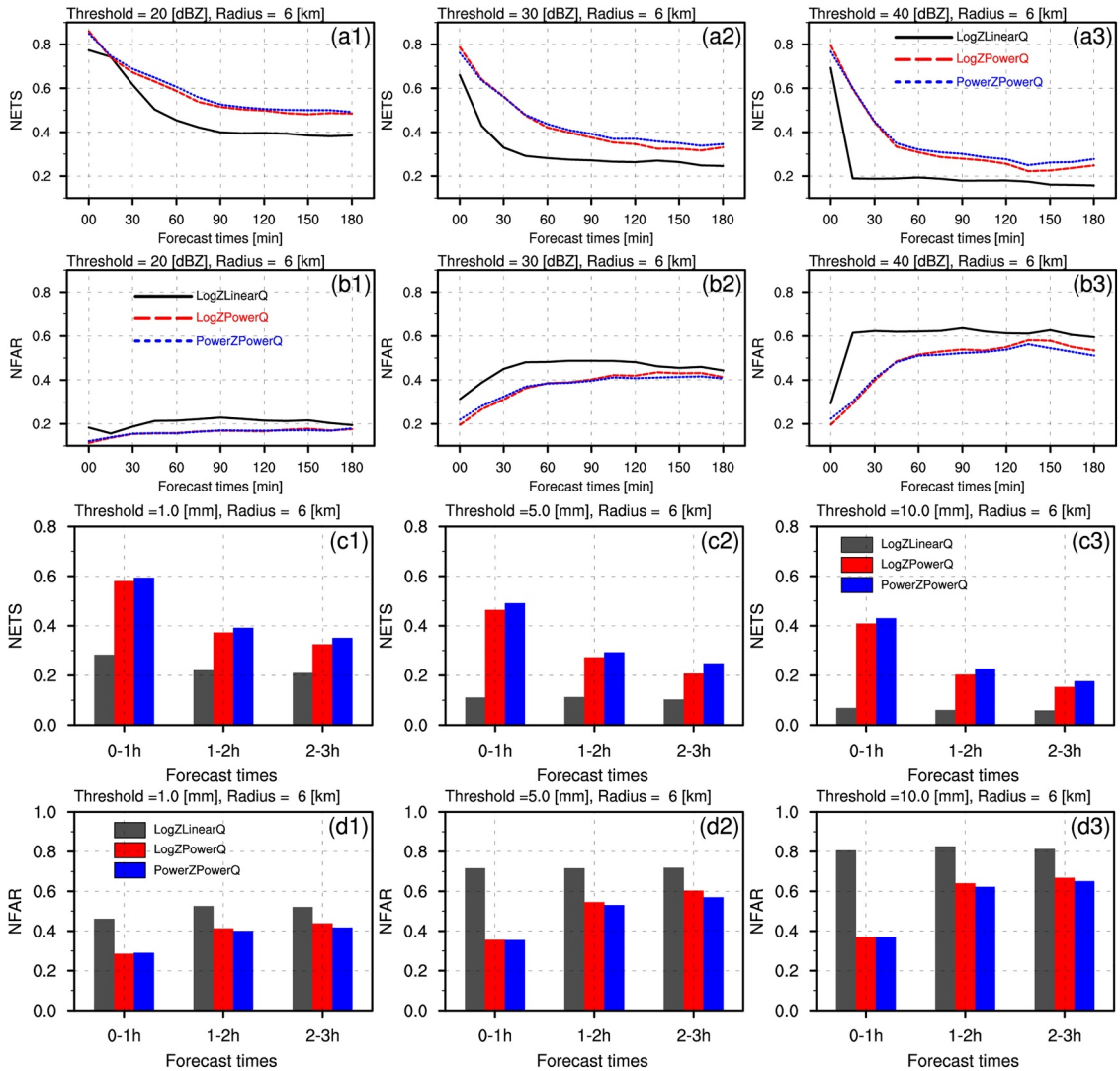

Figure 4. The averaged NETS (a1–a3 and c1–c3) and FAR (b1–b3 and d1–d3) with a 6-km radius over four cycles for 0–3 hr composite reflectivity (a1–b3) and 1-hr accumulated precipitation (c1–d3) forecasts. The thresholds for composite reflectivity and precipitation are 20 dBZ (a1–b1), 30 dBZ (a2–b2), and 40 dBZ (a3–b3), 1.0 mm (c1–d1), 5.0 mm (c2–d2), and 10.0 mm (c3–d3), respectively. LogZLinearQ, LogZPowerQ and PowerZPowerQ are represented by black solid lines/bars, red, and blue dashed lines/bars, respectively.

3.3. Evaluation of Forecast Results Over Other Multiple Cases

To further evaluate the impact of applying the power transformation to both the reflectivity factor and the hydrometeor control variables, multiple other severe convection events with different convective characteristics from the NOAA HWT are also shown in Supporting Information S1. As reported in previous studies (Chen et al., 2021; Hu et al., 2023), the common direct assimilation approach using the original unscaled hydrometeors as control variables to assimilate Z_H exhibits the lowest forecasting skill for all events in both composite reflectivity and precipitation. Overall, the experiments assimilating power-transformed reflectivity factors produce higher forecast skill than those assimilating logarithmic reflectivity factors, with the improvement being more pronounced for precipitation than for composite reflectivity. This is consistent with the results from the single case of 24 May 2019 shown in the previous section. The improvements in PowerZPowerQ are observed in a diverse set of cases including squall lines, clusters of supercells, and mesoscale convective complexes (1, 6, 20, 21, 28 May 2019), which have relatively small model forecast errors. However, for the cases of scattered clusters of strong storms (22, 23 May 2019), which have lower forecast scores throughout the forecast period due to large

model errors, the improvements in PowerZPowerQ over LogZPowerQ are limited. In these cases, PowerZPowerQ's NETS are lower than LogZPowerQ during some periods.

4. Summary and Discussion

Direct assimilation of radar reflectivity is an important approach for improving the initial conditions for convective-scale NWP. However, one of the outstanding challenges is the highly nonlinear relationship between radar reflectivity and the model state variables. Moreover, logarithmically scaled reflectivity factors have been used in all direct assimilation studies to cover the large dynamic measurement range. However, this logarithmic representation amplifies the contribution of small or no-precipitation reflectivity regions and increases the nonlinearity in the radar forward operator, causing reflectivity below a threshold (5–15 dBZ) to need to be filtered out. To alleviate these fundamental and critical problems, this study is the first to document a new approach that simultaneously applies the Box-Cox power transformation to both reflectivity factors and hydrometeor control variables, rather than relying on the long-established approach that links logarithmic reflectivity factors with linear hydrometeor control variables. The new and conventional approaches are compared through a detailed squall line case study and forecast evaluations of multiple severe convective cases from past NOAA HWT Spring Forecast Experiments.

Results from a detailed case analysis show that experiments using the most common assimilation approach utilizing logarithmic reflectivity factors and linear hydrometeor control variables produce the worst forecast performance for composite reflectivity and precipitation due to the high degree of nonlinearity between the observations and control variables. The experiments assimilating logarithmic reflectivity factors using power-transformed hydrometeor control variables provide much better forecast performance, while the newly proposed assimilation approach that applies the power transformation to both reflectivity and hydrometeor control variables exhibits the best overall forecast performance for reflectivity and precipitation. These improvements are mainly attributed to the reduction in nonlinearity of the forward operator after applying nonlinear power transformations to the reflectivity factors and hydrometeor control variables, as well as more reasonable hydrometeor increments from small reflectivity factors, especially for rain. The results from a broader evaluation of different types of convective events show that overall the new assimilation scheme assimilating power-transformed reflectivity demonstrates improved precipitation forecast skill in most convective events, although not as pronounced as in the single case of 24 May 2019.

In the Box-Cox power transformation, the power parameter plays a key role, as it directly influences both the distribution and magnitude of the transformed data, and consequently, the performance of data assimilation. Maximum Likelihood Estimation (MLE) is a typical approach to theoretically estimate the optimal parameters that best fit the data to a Gaussian distribution. However, in practice, the optimal parameters for data assimilation depend not only on the distribution of the transformed data, but also on multiple other factors such as the magnitude of the data and the assumed errors. The parameter that yields a more Gaussian-like distribution (e.g., $p_z = 0.2$) may not necessarily lead to the best assimilation performance. In this study, the power parameters for both the mixing ratios and reflectivity factor were selected based on sensitivity experiments conducted on a limited number of convection events. Therefore, the values adopted here should be regarded as preliminary and further validation with more events is needed.

Lastly, we do not want to limit the idea of applying nonlinear transformations to observations and control variables to mitigate observational operator nonlinearity only to the direct assimilation of radar reflectivity. We believe that for most direct assimilation studies involving nonlinear observation operators, improvements can be achieved by applying appropriate nonlinear transformations to the observations and control variables. This would help reduce the effects of nonlinearities in the operator during the optimal analysis process and regulate/modify the non-Gaussianity in variable error distributions.

Conflict of Interest

The authors declare no conflicts of interest relevant to this study.

Data Availability Statement

For this work, the NEXRAD Level-II data used in this research can be accessed at the National Oceanic and Atmospheric Administration (NOAA) (NOAA, 2019) and also can be downloaded using the AWS service (https://s3.amazonaws.com/noaa-nexrad-level2/index.html#2019/05/) by filling in date and locations of radar site. More information about the NEXRAD radars can be found at https://www.ncei.noaa.gov/products/radar/next-generation-weather-radar. The WRF source code version 3.7.1 (Skamarock et al., 2008) is publicly available at NCAR/UCAR (https://github.com/wrf-model/WRF).

Acknowledgments
This work was supported by the NSF Grants 2136161 and 2527406. Funding was also provided by NOAA/Office of Oceanic and Atmospheric Research under NOAA-University of Oklahoma Cooperative Agreement NA21OAR4320204, U.S. Department of Commerce. Computing for this project was performed at the OU Supercomputing Center for Education and Research (OSCER) at the University of Oklahoma (OU) and the Anvil CPU at Purdue University through allocation EES220057 from the Advanced Cyberinfrastructure Coordination Ecosystem: Services & Support (ACCESS) program, which is supported by National Science Foundation Grants 2138259, 2138286, 2138307, 2137603, and 2138296. The authors would like to extend their gratitude to Dr. Klaus Stephan at the German Weather Service and an anonymous reviewer for providing constructive comments that substantially improved the quality of this manuscript.

References

Aksoy, A., Dowell, D. C., & Snyder, C. (2009). A multicase comparative assessment of the ensemble Kalman filter for assimilation of radar observations. Part I: Storm-scale analyses. *Monthly Weather Review*, *137*(6), 1805–1824. https://doi.org/10.1175/2008MWR2691.1

Blahak, U. (2016). RADAR MIE LM and RADAR MIELIB–calculation of radar reflectivity from model output. In *COSMO Technical Report No. 28. Consortium for Small Scale Modeling*. https://doi.org/10.5676/DWDpub/nwv/cosmo-tr28

Box, G. E. P., & Cox, D. R. (1964). An analysis of transformations. *Journal of the Royal Statistical Society: Series B*, *26*(2), 211–243. https://doi.org/10.1111/j.2517-6161.1964.tb00553.x

Chen, L., Liu, C., Xue, M., Zhao, G., Kong, R., & Jung, Y. (2021). Use of power transform mixing ratios as hydrometeor control variables for direct assimilation of radar reflectivity in GSI En3DVar and tests with five convective storm cases. *Monthly Weather Review*, *149*(3), 645–659. https://doi.org/10.1175/MWR-D-20-0149.1

Clark, A. J., Gallus, W. A., & Weisman, M. L. (2010). Neighborhood-based verification of precipitation forecasts from convection-allowing NCAR WRF Model simulations and the operational NAM. *Weather and Forecasting*, *25*(5), 1495–1509. https://doi.org/10.1175/2010WAF2222404.1

Clark, A. J., Jirak, I. L., Gallo, B. T., Roberts, B., Knopfmeier, K. H., Clark, R. A., et al. (2020). A real-time, simulated forecasting experiment for advancing the prediction of hazardous convective weather. *Bulletin of the American Meteorological Society*, *101*(11), E2022–E2024. https://doi.org/10.1175/BAMS-D-19-0298.1

Dowell, D. C., Alexander, C. R., James, E. P., Weygandt, S. S., Benjamin, S. G., Manikin, G. S., et al. (2022). The high-resolution rapid refresh (HRRR): An hourly updating convection-allowing forecast model. Part I: Motivation and system description. *Weather and Forecasting*, *37*(8), 1371–1395. https://doi.org/10.1175/WAF-D-21-0151.1

Gan, R., Yang, Y., Li, H., Guo, S., Xie, Q., & Liu, P. (2023). An economical assimilation scheme for radar reflectivity in non-convective region to suppress spurious precipitation. *Quarterly Journal of the Royal Meteorological Society*, *149*(757), 3525–3540. https://doi.org/10.1002/qj.4571

Gao, J. (2017). A three-dimensional variational radar data assimilation scheme developed for convective scale NWP. In S. K. Park & L. Xu (Eds.), *Data assimilation for atmospheric, oceanic and hydrologic applications* (Vol. III, pp. 285–326). Springer International Publishing. Cham. https://doi.org/10.1007/978-3-319-43415-5_13

Gao, J., Fu, C., Stensrud, D. J., & Kain, J. S. (2016). OSSEs for an ensemble 3DVAR data assimilation system with radar observations of convective storms. *Journal of the Atmospheric Sciences*, *73*(6), 2403–2426. https://doi.org/10.1175/JAS-D-15-0311.1

Gao, J., Heinselman, P. L., Xue, M., Wicker, L. J., Yussouf, N., Stensrud, D. J., & Droegemeier, K. K. (2024). The numerical prediction of severe convective storms: Advances in research and applications, remaining challenges, and outlook for the future. In *Reference module in Earth systems and environmental sciences*. Elsevier. https://doi.org/10.1016/B978-0-323-96026-7.00127-2

Gao, J., Smith, T. M., Stensrud, D. J., Fu, C., Calhoun, K., Manross, K. L., et al. (2013). A real-time weather-adaptive 3DVAR analysis system for severe weather detections and warnings. *Weather and Forecasting*, *28*(3), 727–745. https://doi.org/10.1175/WAF-D-12-00093.1

Gao, J., & Stensrud, D. J. (2012). Assimilation of reflectivity data in a convective-scale, cycled 3DVAR framework with hydrometeor classification. *Journal of the Atmospheric Sciences*, *69*(3), 1054–1065. https://doi.org/10.1175/JAS-D-11-0162.1

Gao, J., Xue, M., Brewster, K., & Droegemeier, K. K. (2004). A three-dimensional variational data analysis method with recursive filter for Doppler radars. *Journal of Atmospheric and Oceanic Technology*, *21*(3), 457–469. https://doi.org/10.1175/1520-0426(2004)021<0457:ATVDAM>2.0.CO;2

Gao, J., Xue, M., Shapiro, A., & Droegemeier, K. K. (1999). A variational method for the analysis of three-dimensional wind fields from two Doppler radars. *Monthly Weather Review*, *127*(9), 2128–2142. https://doi.org/10.1175/1520-0493(1999)127<2128:AVMFTA>2.0.CO;2

Han, B., Fan, J., Varble, A., Morrison, H., Williams, C. R., Chen, B., et al. (2019). Cloud-resolving model intercomparison of an MC3E squall line case: Part II. Stratiform precipitation properties. *Journal of Geophysical Research: Atmospheres*, *124*(2), 1090–1117. https://doi.org/10.1029/2018JD029596

Hu, J., Gao, J., Liu, C., Zhang, G., Heinselman, P., & Carlin, J. T. (2023). Test of power transformation function to hydrometeor and water vapor mixing ratios for direct variational assimilation of radar reflectivity data. *Weather and Forecasting*, *38*(10), 1995–2010. https://doi.org/10.1175/WAF-D-22-0158.1

Janjić, T., & Zeng, Y. (2021). Weakly constrained LETKF for estimation of hydrometeor variables in convective-scale data assimilation. *Geophysical Research Letters*, *48*(24), e2021GL094962. https://doi.org/10.1029/2021gl094962

Jung, Y., Zhang, G., & Xue, M. (2008). Assimilation of simulated polarimetric radar data for a convective storm using the ensemble Kalman filter. Part I: Observation operators for reflectivity and polarimetric variables. *Monthly Weather Review*, *136*(6), 2228–2245. https://doi.org/10.1175/2007mwr2083.1

Lai, A., Gao, J., Koch, S. E., Wang, Y., Pan, S., Fierro, A. O., et al. (2019). Assimilation of radar radial velocity, reflectivity, and pseudo–water vapor for convective-scale NWP in a variational framework. *Monthly Weather Review*, *147*(8), 2877–2900. https://doi.org/10.1175/MWR-D-18-0403.1

Li, H., Liu, C., Xue, M., Park, J., Chen, L., Jung, Y., et al. (2022). Use of power transform total number concentration as control variable for direct assimilation of radar reflectivity in GSI En3DVar and tests with six convective storms cases. *Monthly Weather Review*, *150*(4), 821–842. https://doi.org/10.1175/MWR-D-21-0041.1

Liu, P., Gao, J., Zhang, G., & Carlin, J. T. (2024). Assimilation of radar reflectivity data using parameterized forward operators for improving short-term forecasts of high-impact convection events. *Journal of Geophysical Research: Atmospheres*, *129*(20), e2024JD041458. https://doi.org/10.1029/2024JD041458

Liu, P., Zhang, G., Carlin, J. T., & Gao, J. (2024). A new melting model and its implementation in parameterized forward operators for polarimetric radar data simulation with double moment microphysics schemes. *Journal of Geophysical Research: Atmospheres*, *129*(9), e2023JD040026. https://doi.org/10.1029/2023JD040026

Mahale, V. N., Zhang, G., Xue, M., Gao, J., & Reeves, H. D. (2019). Variational retrieval of rain microphysics and related parameters from polarimetric radar data with a parameterized operator. *Journal of Atmospheric and Oceanic Technology*, *36*(12), 2483–2500. https://doi.org/10.1175/jtech-d-18-0212.1

Morrison, H., Milbrandt, J. A., Bryan, G. H., Ikeda, K., Tessendorf, S. A., & Thompson, G. (2015). Parameterization of cloud microphysics based on the prediction of bulk ice particle properties. Part II: Case study comparisons with observations and other schemes. *Journal of the Atmospheric Sciences*, *72*(1), 312–339. https://doi.org/10.1175/JAS-D-14-0066.1

Morrison, H., Thompson, G., & Tatarskii, V. (2009). Impact of cloud microphysics on the development of trailing stratiform precipitation in a simulated squall line: Comparison of one-and two-moment schemes. *Monthly Weather Review*, *137*(3), 991–1007. https://doi.org/10.1175/2008mwr2556.1

National Oceanic and Atmospheric Administration (NOAA). (2019). The Next Generation Weather Radar (NEXRAD) Level-II data [Dataset]. Retrieved from https://s3.amazonaws.com/noaa-nexrad-level2/index.html#2019/05/

Schwartz, C. S. (2017). A comparison of methods used to populate neighborhood-based contingency tables for high-resolution forecast verification. *Weather and Forecasting*, *32*(2), 733–741. https://doi.org/10.1175/WAF-D-16-0187.1

Skamarock, W. C., Klemp, J. B., Dudhia, J., Gill, D. O., Barker, D. M., Duda, M. G., et al. (2008). A description of the advanced research WRF version 3 (No. NCAR/TN-475+STR) [Software], *475*, 113. https://doi.org/10.5065/D68S4MVH

Tong, M., & Xue, M. (2005). Ensemble Kalman filter assimilation of Doppler radar data with a compressible nonhydrostatic model: OSS experiments. *Monthly Weather Review*, *133*(7), 1789–1807. https://doi.org/10.1175/MWR2898.1

Varble, A., Zipser, E. J., Fridlind, A. M., Zhu, P., Ackerman, A. S., Chaboureau, J.-P., et al. (2014). Evaluation of cloud-resolving and limited area model intercomparison simulations using TWP-ICE observations: 2. Precipitation microphysics. *Journal of Geophysical Research: Atmospheres*, *119*(24), 13919–13945. https://doi.org/10.1002/2013JD021372

Wang, H., Sun, J., Fan, S., & Huang, X.-Y. (2013). Indirect assimilation of radar reflectivity with WRF 3D-Var and its impact on prediction of four summertime convective events. *Journal of Applied Meteorology and Climatology*, *52*(4), 889–902. https://doi.org/10.1175/JAMC-D-12-0120.1

Wolfensberger, D., & Berne, A. (2018). From model to radar variables: A new forward polarimetric radar operator for COSMO. *Atmospheric Measurement Techniques*, *11*(7), 3883–3916. https://doi.org/10.5194/amt-11-3883-2018

Yang, R., Purser, R. J., Carley, J. R., Pondeca, M., Zhu, Y., & Levine, S. (2020). Application of a nonlinear transformation function to the variational analysis of visibility and ceiling height. *NOAA/NCEP Office Note*, *502*. https://doi.org/10.25923/esw8-5n84

Zhang, G. (2016). *Weather radar polarimetry* (1st ed.). CRC Press. https://doi.org/10.1201/9781315374666

Zhang, G., Gao, J., & Du, M. (2021). Parameterized forward operators for simulation and assimilation of polarimetric radar data with numerical weather predictions. *Advances in Atmospheric Sciences*, *38*(5), 737–754. https://doi.org/10.1007/s00376-021-0289-6

References From the Supporting Information

Hong, S.-Y., Noh, Y., & Dudhia, J. (2006). A new vertical diffusion package with an explicit treatment of entrainment processes. *Monthly Weather Review*, *134*(9), 2318–2341. https://doi.org/10.1175/MWR3199.1

Iacono, M. J., Delamere, J. S., Mlawer, E. J., Shephard, M. W., Clough, S. A., & Collins, W. D. (2008). Radiative forcing by long-lived greenhouse gases: Calculations with the AER radiative transfer models. *Journal of Geophysical Research*, *113*(D13). https://doi.org/10.1029/2008JD009944

Liu, C., Xue, M., & Kong, R. (2019). Direct assimilation of radar reflectivity data using 3DVAR: Treatment of hydrometeor background errors and OSSE tests. *Monthly Weather Review*, *147*(1), 17–29. https://doi.org/10.1175/MWR-D-18-0033.1

Milbrandt, J., & Yau, M. (2005a). A multimoment bulk microphysics parameterization. Part I: Analysis of the role of the spectral shape parameter. *Journal of the Atmospheric Sciences*, *62*(9), 3051–3064. https://doi.org/10.1175/jas3534.1

Milbrandt, J., & Yau, M. (2005b). A multimoment bulk microphysics parameterization. Part II: A proposed three-moment closure and scheme description. *Journal of the Atmospheric Sciences*, *62*(9), 3065–3081. https://doi.org/10.1175/jas3535.1

Purser, R. J., Wu, W.-S., Parrish, D. F., & Roberts, N. M. (2003). Numerical aspects of the application of recursive filters to variational statistical analysis. Part I: Spatially homogeneous and isotropic Gaussian covariances. *Monthly Weather Review*, *131*(8), 1524–1535. https://doi.org/10.1175/1520-0493(2003)131<1524:NAOTAO>2.0.CO;2